Electronic Spectra and Crystal Field Analysis of Er3+ in Cs2NaErF6

3 **AUTHORS**, INCLUDING:

Xianju Zhou
Chongqing University of Posts and Telecom…
59 PUBLICATIONS   **317** CITATIONS

Peter Anthony Tanner
The Hong Kong Institute of Education
355 PUBLICATIONS   **4,362** CITATIONS

Electronic Spectra and Crystal Field Analysis of Er³⁺ in Cs₂NaErF₆

Xianju Zhou,[†,‡] **Peter A. Tanner,**[*,‡] **and Michèle D. Faucher**[§]

Institute of Modern Physics, Chongqing University of Post and Telecommunications, Chongqing 400065, Department of Biology and Chemistry, City University of Hong Kong, Tat Chee Avenue, Kowloon, Hong Kong S.A.R., P.R. China, and 88 Avenue Jean Jaurès, 92140 Clamart, France

The optical electronic spectra of Cs₂NaErF₆, Cs₂NaY₀.₉Er₀.₁F₆, and Cs₂NaM₀.₅Er₀.₅F₆ (M = Sc, Ga) have been investigated at temperatures down to 10 K. The absorption spectra span the range from 6000 to 41 000 cm⁻¹, whereas emission has been observed from the ⁴S₃/₂, ⁴F₉/₂, ⁴I₉/₂, and ⁴I₁₁/₂ multiplet terms in the spectral range from 25 000 to 9000 cm⁻¹. Each transition between crystal field levels comprises extensive, well-resolved vibronic structure. From the detailed vibronic analyses, 39 crystal field levels have been assigned from 0 to 27 642 cm⁻¹. A configuration interaction assisted crystal field (CIACF) calculation provides a good energy level fit with reasonable energy parameters. The mean deviation of the standard 4f¹¹2p⁶ fit to the energy levels (23 cm⁻¹) exceeded that for the 4f¹¹2p⁶/4f¹²2p⁵ CIACF fitting (6.4 cm⁻¹), which provides 4f¹¹2p⁶/4f¹²2p⁵ further evidence for the importance of the charge-transfer configuration interaction.

1. Introduction

Although the electronic spectra of Cs₂NaLnCl₆ (Ln = Ce...Yb) have been studied extensively,[1] there have been fewer reports for Cs₂NaLnF₆ systems (e.g., see refs 2−5). However, the use of two-photon spectroscopy by Denning et al. has enabled comprehensive energy level datasets to be achieved in some cases.[6,7] The Cs₂NaLnF₆ systems are interesting because they are harder, less moisture-sensitive crystals and may be exploited for technological uses. From a theoretical viewpoint, the greater crystal field strength for the hexafluoroelpasolite crystals produces a tough test for crystal field energy level calculations because only two parameters are employed to model the crystal field in these LnF₆³⁻ octahedral symmetry systems.

Recently, Makhov et al.[8] have reported the vacuum-ultraviolet emission and excitation spectra of Cs₂NaYF₆ doped with Er³⁺ and focused upon the d−f transitions, although emission from the f-electron multiplet terms ²F(2)₇/₂, ²P₃/₂, and ⁴S₃/₂ was assigned. In the present study, we aim to provide a complete description of the lower energy electronic spectra of Er³⁺ in hexafluoroelpasolite hosts and to derive the electronic energy level diagram. The fitting of the energy levels of Er³⁺ in Cs₂NaErCl₆ has been shown to be considerably improved if the interaction with the charge-transfer configuration 4f¹²3p⁵ is included.[9] We anticipated that such an interaction might be less important for Er³⁺ in Cs₂NaErF₆ because the interacting configuration is then at higher energy, whereas intraconfiguration interactions are greater because of the stronger crystal field. One of the major motivations of the present study was to test if this is so.

2. Experimental

Chemical Preparation. Samples of Cs₂NaErF₆, Cs₂NaYF₆:Er³⁺ (10 atom %), and Cs₂NaMF₆:Er³⁺ (50 atom %) (M = Sc,

Ga) were purchased from N. M. Khaidukov, who synthesized them by the hydrothermal method.[5] The crystals were colorless and transparent and measured several mm by 1 mm thickness. They were used in the optical experiments without further preparation.

Instrumentation. Electronic absorption spectra were obtained at the resolution 2 cm⁻¹ by a Biorad FTS-60A spectrometer, equipped with DTGS, PbSe, Si, and photomultiplier tube detectors, in the region of 1000 to 28 000 cm⁻¹. The ultraviolet spectra (up to 40 000 cm⁻¹) were recorded as single-beam spectra at a resolution of between 2 and 4 cm⁻¹ by an Acton 0.5 m monochromator, having an 1800 groove mm⁻¹ grating blazed at 250 nm, and a back-illuminated SpectruMM charge-coupled device (CCD) detector, using deuterium (D₂) or xenon (Xe) lamps as the external light source. All the spectra were recorded between 300 and 10 K with the polished sample housed in an Oxford Instruments closed cycle cryostat.

Emission spectra were recorded at temperatures down to 10 K using a tunable pulsed laser (Panther OPO system pumped by the third harmonic of a Surelite Nd:YAG laser). The signal was collected at 90° by an Acton 0.5 m monochromator with gratings blazed at 250 nm (1800 groove mm⁻¹), 500 nm (1200 groove mm⁻¹), and 750 nm (600 groove mm⁻¹), respectively, and a back-illuminated SpectruMM CCD detector.

3. Results and Discussion

Electronic Spectra. The electronic configuration of Er³⁺ is 4f¹¹ and because this ion in Cs₂NaErF₆ and Cs₂NaYF₆:Er³⁺ occupies a site of octahedral symmetry, these electronic states are classified under the *O** double group in which all crystal field levels are of ungerade parity. The site selection rules for electronic spectra potentially enable magnetic dipole transitions between all states (except those between Γ₆ and Γ₇ states), and analogously to the corresponding chloro- systems, one ungerade phonon vibronic sidebands are electric dipole allowed.[1]

We have recorded the electronic absorption spectra in the range from 6000 cm⁻¹ to 41 000 cm⁻¹ at ∼10, 77, and 150 K. The transitions from the electronic ground state, ⁴I₁₅/₂aΓ₈ to the

* Corresponding author. E-mail: bhtan@cityu.edu.hk.
† Chongqing University of Post and Telecommunications.
‡ City University of Hong Kong.
§ 88 Avenue Jean Jaurès.

TABLE 1: Experimental and Calculated Energy Levels (in cm^{-1}) for Er^{3+} in Cs$_2$NaErCl$_6$ and Cs$_2$NaErF$_6$

			Cs$_2$NaErCl$_6$			Cs$_2$NaErF$_6$						Cs$_2$NaErCl$_6$			Cs$_2$NaErF$_6$		
level	SLJ	IR^a	exp^b	calc	Δ	exp	calc	Δ	level	SLJ	IR^a	exp^b	calc	Δ	exp	calc	Δ
1	$^4I_{15/2}$	$a\Gamma_8$	0	4	−4	0	8	−8	45		Γ_6	27775	27759	16		28033	
2		Γ_7	25	27	−2	65	64	1	46		$c\Gamma_8$		27760			28060	
3		$b\Gamma_8$	57	61	−4	113	114	−1	47	$^4G_{7/2}$	Γ_7		27864			28147	
4		Γ_6	259	261	−2	488	489	−1	48	$^2K_{15/2}$	Γ_8	(27966)	27955	11		28366	
5		$c\Gamma_8$	287	293	−6	537	539	−2	49		Γ_6	(27981)	27989	−8		28434	
6	$^4I_{13/2}$	Γ_6	6492	6481	11	6510	6510	0	50	$^2P_{3/2}$	Γ_8	31367	31375	−8			
7		$a\Gamma_8$	6517	6507	10	6552	6551	1	51	$^2K_{13/2}$	Γ_6	32613	32608	5			
8		$a\Gamma_7$	6532	6521	11	6586	6581	5	52		Γ_8	32676	32676	0			
9		$b\Gamma_8$	6682	6670	12	6883	6866	17	53		Γ_7		32739				
10		$b\Gamma_7$	6686	6676	10	6883	6877	6	54	$^2P_{1/2}$	Γ_6		32921				
11	$^4I_{11/2}$	Γ_6	10166	10168	−2	10227	10234	−7	55	$^4G_{5/2}$	Γ_8		32930				
12		$a\Gamma_8$	10174	10177	−3	10243	10248	−5	56	$^2K_{13/2}$	Γ_7		32999				
13		Γ_7	10238	10244	−6	10384	10390	−6	57		Γ_8		33076				
14		$b\Gamma_8$	10238	10245	−7	10384	10394	−10	58	$^4G_{5/2}$	Γ_7		33210				
15	$^4I_{9/2}$	$a\Gamma_8$	12357	12352	5	12409	12397	12	59	$^4G_{7/2}$	Γ_6	(33750)	33731	19			
16		Γ_6	12422	12436	−14	12561	12566	−5	60		Γ_8	(33794)	33811	−17			
17		$b\Gamma_8$	12502	12512	−10	12683	12679	4	61		Γ_7	(33908)	33944	−36			
18	$^4F_{9/2}$	$a\Gamma_8$	15152	15150	2	15241	15237	4	62	$^2D(1)_{5/2}$	Γ_7	(34552)	34564	−12			
19		$b\Gamma_8$	15246	15248	−2	15412	15426	−14	63		Γ_8	34635	34644	−9			
20		Γ_6	15337	15340	−3	15574	15576	−2	64	$^2H(2)_{9/2}$	$a\Gamma_8$	36224	36218	6			
21	$^4S_{3/2}$	Γ_8	18265	18264	1	18316	18316	0	65		Γ_6	36309	36308	1			
22	$^2H(2)_{11/2}$	$a\Gamma_8$	19010	19011	−1	19212	19204	8	66		$b\Gamma_8$	(36412)	36410	2			
23		Γ_7	19048	19054	−6	19219	19214	5	67	$^4D_{5/2}$	Γ_7	38164	38157	7			
24		$b\Gamma_8$	19137	19132	5	19351	19350	1	68		Γ_8	38234	38231	3			
25		Γ_6	19174	19171	3	19413	19411	2	69	$^4D_{7/2}$	Γ_6	38705	38712	−7			
26	$^4F_{7/2}$	Γ_6	20374	20368	6	20527	20516	11	70		Γ_8	38790	38806	−16			
27		Γ_8	20446	20442	4	20629	20628	1	71		Γ_7	38993	38979	14			
28		Γ_7	20467	20462	5	20640	20641	−1	72	$^2I_{11/2}$	Γ_7	40668	40659	9			
29	$^4F_{5/2}$	Γ_8	22056	22058	−2	22216	22225	−9	73		$a\Gamma_8$		40718				
30		Γ_7	22135	22145	−10		22388		74		Γ_6	(40750)	40749	1			
31	$^4F_{3/2}$	Γ_8	22445	22443	2	22642	22641	1	75		$b\Gamma_8$	(40815)	40791	24			
32	$^2G_{9/2} + {}^4F_{9/2}$	$a\Gamma_8$	24425	24410	15	24518	24511	7	76	$^2L_{17/2}$	Γ_6	(41187)	41184	3			
33		Γ_6	24459	24455	4	24633	24634	−1	77		$a\Gamma_8$	(41194)	41185	9			
34		$b\Gamma_8$	24519	24512	7	24690	24693	−3	78		$a\Gamma_7$		41264				
35	$^4G_{11/2}$	$a\Gamma_8$	26098	26105	−7	26225	26230	−5	79		$b\Gamma_8$		41266				
36		Γ_7	26183	26195	−12	26371	26380	−9	80		$b\Gamma_6$	(41270)	41267	3			
37		$b\Gamma_8$	26354	26361	−7	26618	26620	−2	81		$c\Gamma_8$		41278				
38		Γ_6	26408	26418	−10	26738	26731	7	82	$^4D_{3/2}$	Γ_8	41965	41963	2			
39	$^4G_{9/2}$	Γ_6	(27179)	27167	12		27373		83	$^2P_{3/2}$	Γ_8	(42518)	42539	−21			
40	$^4G_{9/2} + {}^2K_{15/2}$	$a\Gamma_8$	27220	27211	9	27434	27430	4	84	$^2I_{13/2}$	$a\Gamma_7$	(43034)	43039	−5			
41		$b\Gamma_8$	27259	27252	7	27462	27461	1	85		$a\Gamma_8$	(43048)	43044	4			
42		$a\Gamma_8$	27365	27368	−3		27555		86		$b\Gamma_7$	(43290)	43304	−14			
43		$b\Gamma_8$	27459	27478	−19		27633		87		$b\Gamma_8$	(43362)	43339	23			
44		Γ_7	27504^c	27591			27754		88		Γ_6	43388	43394	−6			

^{a} Irreducible representation in O_h molecular point group symmetry. ^{b} Experimental energy. ^{c} Removed from the dataset.

higher multiplet terms ^4I_J ($2J$ = 13, 11, 9), ^4F_J ($2J$ = 9, 7, 5, 3), $^4S_{3/2}$, $^2H(2)_{11/2}$, $^2G_{9/2}$, and $^4G_{11/2}$ were recorded and assigned. The derived energy levels are listed in Table 1. A selection of the spectra is shown in Figure 1a−c. Other than the transition $^4I_{15/2} \rightarrow {}^4I_{13/2}$ transition (Figure 1a) which comprises mostly magnetic dipole intensity, the remaining transitions are mainly vibronic in character. The three zero phonon lines in Figure 1a are assigned to transitions to the terminal $^4I_{13/2}\Gamma_6,a\Gamma_8,a\Gamma_7$ crystal field levels in order of increasing energy. The starred bands represent hot transitions from the first excited $^4I_{15/2}$ state at 66 ± 1 cm^{-1}. The transitions to the two upper $^4I_{13/2}$ levels are too weak to be distinguished from noise.

The vibronic structure of the transitions is now briefly described because it is richer than in Cs$_2$NaErCl$_6$ due to greater dispersion in Cs$_2$NaErF$_6$, and it provides conclusive identification and assignment of the locations of electronic origins. In particular, the structure of the $^4I_{15/2}a\Gamma_8 \rightarrow {}^4S_{3/2}a\Gamma_8$ transition (Figure 1b) is well resolved because there are no overlapping electronic transitions. The zero phonon line is marked 0 in Figure 1b, and the displacements of other bands from the zero phonon line are indicated. Also marked in the figure are the unit cell group modes that have similar energies to the vibronic peak

displacements. In this transition, the S$_7$ vibronic origin is more intense than S$_{10}$, just as for Cs$_2$NaErCl$_6$.

Figure 1c shows the intense $^4I_{15/2}a\Gamma_8 \rightarrow {}^2H(2)_{11/2}$ transition. Four electronic transitions are identified among which two zero phonon lines are directly observed in Figure 1c. The detailed assignments are collected in Table 2.

Selected emission spectra are shown in Figure 2. Under 355 nm excitation, in the region between 25 000 and 9300 cm^{-1}, emission is observed from $^4S_{3/2}$, $^4F_{9/2}$, $^4I_{9/2}$, and $^4I_{11/2}$ initial multiplet terms that not only confirms the assignment of the lowest crystal field state of these multiplets but also enables the crystal field levels of the $^4I_{15/2}$ ground state to be assigned. All spectral features have been assigned in these spectra. The major bands in the $^4S_{3/2}\Gamma_8 \rightarrow {}^4I_{15/2}$ transition at 10 K are labeled in Figure 2a according to the nature of the terminal level. The transition to the $^4I_{13/2}$ multiplet (see Figure 2b) comprises mostly magnetic dipole intensity, and it enables the upper $^4I_{13/2}b\Gamma_8,\Gamma_7$ crystal field levels to be assigned in a corresponding manner as the spectrum of Cs$_2$NaErCl$_6$.

The emission spectra of Cs$_2$NaYF$_6$:Er^{3+} (10 atom %) were assigned analogously and the vibronic peaks exhibit less dispersion. The emission spectra of Cs$_2$NaMF$_6$:Er^{3+} (M = Sc,
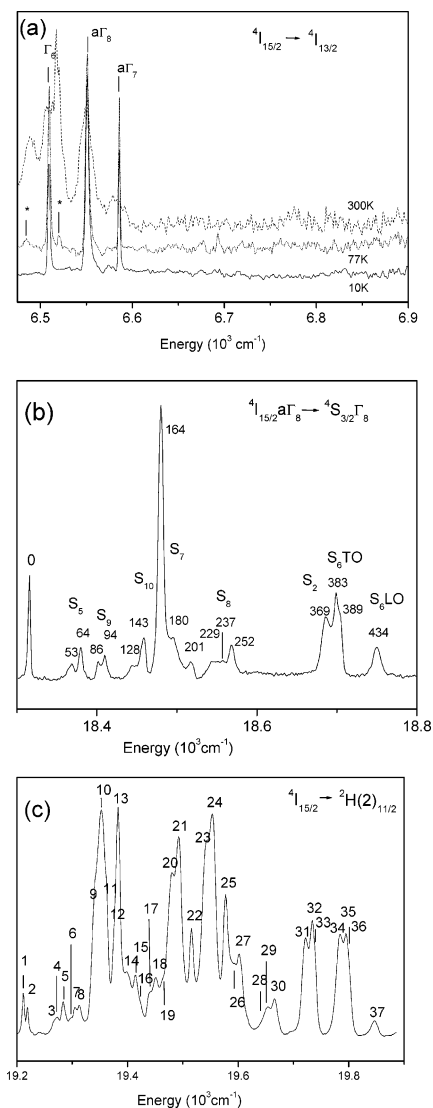
Spectra and Analysis of Er^{3+} in Cs$_2$NaErF$_6$

J. Phys. Chem. C, Vol. 111, No. 2, 2007 **685**

Figure 1. Selected absorption spectra of Cs$_2$NaErF$_6$ between: (a) 6470−6900 cm^{-1} at the indicated temperatures; (b) 18 300−18 800 cm^{-1} at 10 K; and (c) 19 200−19 900 cm^{-1} at 10 K. The ordinate in all cases is absorption. The starred bands in (a) are hot electronic transitions. The vibrational energy displacements from the zero phonon line (0) are marked in (b). The assignments for (c) are collected in Table 2.

Ga; 50 atom %) exhibit two sites so that zero phonon lines are split by energies between 3 and 7 cm^{-1}.

Crystal Field Analyses. The 39 experimentally determined energy levels of Cs$_2$NaErF$_6$ were fitted by two methods: (i) utilizing a standard Hamiltonian in the 4f^{11}2p^6 configuration (with 2p^6 representing a closed ligand shell of p electrons) and (ii) the same Hamiltonian corrected for the effects of configuration interaction with 4f^{12}2p^5 in which the lanthanide ion has gained an electron, and the ligand shell has lost one. We abbreviate the latter analysis as the configuration interaction assisted crystal field (CIACF) calculation. The standard Hamiltonian involves 16 free-ion parameters: E_{ave}, the mean energy of the configuration; the Slater parameters F^k ($k = 2, 4, 6$); the configuration interaction parameters, α, β, and γ; the three body parameters T^i ($i = 2, 3, 4, 6, 7, 8$); the parameters of magnetic interactions M^k ($k = 0$ (2, 4); $M^2 = 0.56\ M^0$; $M^4 = 0.38\ M^0$) and P^k ($k = 2$ (4, 6); $P^4 = 0.75\ P^2$; $P^6 = 0.5\ P^2$); and the spin orbit coupling constant, ζ_f. Actually, because of the limited number of high-lying levels, T^8 was not fitted but was ascribed a plausible value. Besides, two crystal field parameters are

TABLE 2: $^4I_{15/2}a\Gamma_8 \rightarrow\ ^2H(2)_{11/2}$ Absorption Spectrum of Cs$_2$NaErF$_6$ at 10 K

line[a]	energy (cm^{-1})[b]	assignment of upper level, $^2H(2)_{11/2}$[c]
1	19212mw	aΓ_8
2	19219w	Γ_7
3	19266sh	aΓ_8 + S$_5$(54)
4	19273w	aΓ_8 + S$_5$(61); Γ_7 + S$_5$(54)
5	19284w	Γ_7 + S$_5$(65)
6	19298sh	aΓ_8 + S$_9$(86)
7	19305w	aΓ_8 + S$_9$(93); Γ_7 + S$_9$(86)
8	19313w	Γ_7 + S$_9$(94)
9	19339sh	aΓ_8 + S$_{10}$(127)
10	19352s	aΓ_8 + S$_{10}$(140); bΓ_8
11	19363sh	Γ_7 + S$_{10}$(144)
12	19375sh	aΓ_8 + S$_7$(163)
13	19383s	Γ_7 + S$_7$(164)
14	19401w	Γ_7 + S$_7$(182); bΓ_8 + S$_5$(50)
15	19415w	aΓ_8 + S$_7$(203); bΓ_8 + S$_5$(64)
16	19423sh	Γ_7 + S$_7$(204)
17	19438sh	aΓ_8 + S$_8$(226); bΓ_8 + S$_9$(87)
18	19451w	aΓ_8 + S$_8$(239)
19	19463sh	aΓ_8 + S$_8$(251); Γ_7 + S$_8$(244); Γ_6 + S$_5$(50)
20	19479s	bΓ_8 + S$_{10}$(128)
21	19493s	bΓ_8 + S$_{10}$(142)
22	19516ms	bΓ_8 + S$_7$(165)
23	19541s	Γ_6 + S$_{10}$(128)
24	19553s	Γ_6 + S$_{10}$(140)
25	19577s	Γ_6 + S$_7$(164)
26	19592m	aΓ_8 + S$_6$(380); Γ_6 + S$_7$(179)
27	19602m	aΓ_8 + S$_6$(390); Γ_7 + S$_6$(383)
28	19645sh	aΓ_8 + S$_6$(433); Γ_6 + S$_8$(232)
29	19652mw	Γ_7 + S$_6$(433); Γ_6 + S$_8$(239)
30	19666m	Γ_6 + S$_8$(253)
31	19722ms	bΓ_8 + S$_6$(371)
32	19734ms	bΓ_8 + S$_6$(383)
33	19738sh	bΓ_8 + S$_6$(387)
34	19784ms	bΓ_8 + S$_6$(433); Γ_6 + S$_6$(371)
35	19795ms	Γ_6 + S$_6$(382)
36	19801sh	Γ_6 + S$_6$(388)
37	19847mw	Γ_6 + S$_6$(434)

[a] Figure 1c. [b]sh shoulder; w weak; v very; m medium; s strong. [c]The Cs$_2$NaErF$_6$ vibronic displacements are given in parentheses and are compared with the unit cell group modes with energies as in Figure 1b. The electronic states aΓ_8, Γ_7, bΓ_8, Γ_6 are assigned (in cm^{-1}) at 19212, 19219, 19351, 19413.

required in octahedral symmetry: B_0^4 and B_0^6 with $B_4^4 = \pm\ B_0^4$ $(5/14)^{1/2}$ and $B_4^6 = \mp\ B_0^6\ (7/2)^{1/2}$. The special case of the configuration interaction 4f^{N}np^6/4f^{N+1}np^5 utilized here was previously discussed for the cases of Cs$_2$NaTmCl$_6$[9] and Cs$_2$NaErCl$_6$[10] in which it led to a dramatic decrease of the deviation between experimental and calculated energies. The inclusion of configuration interaction requires four more parameters: (i) the spin−orbit coupling constant ζ(2p); (ii) the multiplier X of the interconfiguration parameters R^k (the hybrid integrals R^2(f,f,f,p), R^4(f,f,f,p) and R^2(f,p,p,p) are relevant); (iii) the crystal field parameter B_0^4 (4f2p); and (iv) the mean energy of the excited configuration E'_{ave} with respect to 4f^{11}. The value of ζ(2p) was fixed herein to 500 cm^{-1}, which is the value for a 2p electron in neon 2p^6. The fitted value of X was 0.267, which is nearly twice the magnitude of that for Er^{3+} in Cs$_2$NaErCl$_6$, so that R^2(f,f,f,p) = −4575 cm^{-1} and R^4(f,f,f,p) = −2234 cm^{-1}. Actually, this parameter is loosely determined because the other parameters adjust themselves in such a way that the lowest levels of the excited configuration 4f^{12}2p^5 ($^4H_{13/2}$) are situated close to 54 000 cm^{-1}, which is about 2000 cm^{-1} above $^2H_{11/2}$ (4f^{11}).

Thus, the total number of parameters employed for the 4f^{11}2p^6 analysis was 17, whereas 20 were employed for 4f^{11}2p^6/4f^{12}2p^5. Although this is quite a large number, it is interesting to note that the final mean deviations are 23 and 6.4

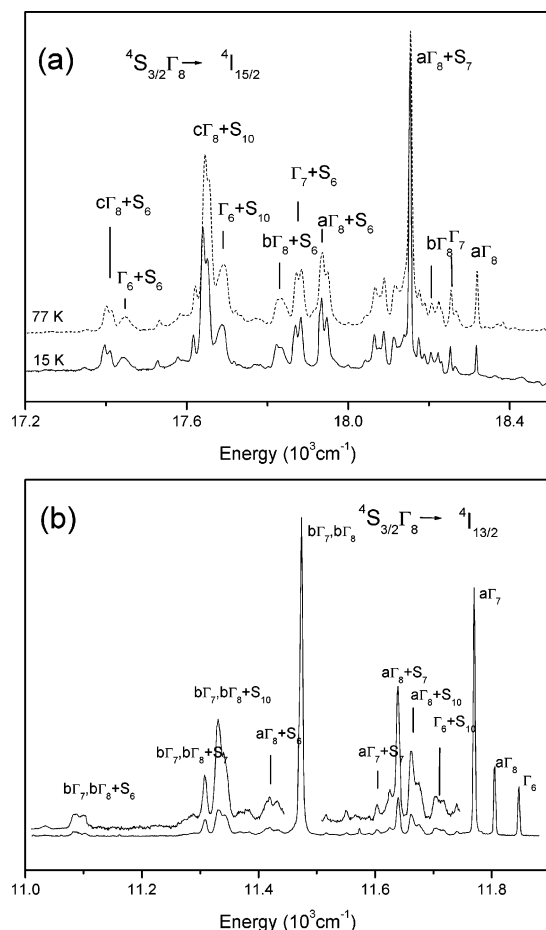**Figure 2.** Selected 355 nm excited emission spectra of Cs_2NaErF_6: (a) between 18 500 and 17 400 cm^{-1} at the temperatures indicated; (b) between 11870 and 11 000 cm^{-1} at 10 K. The ordinate in both cases is emission.
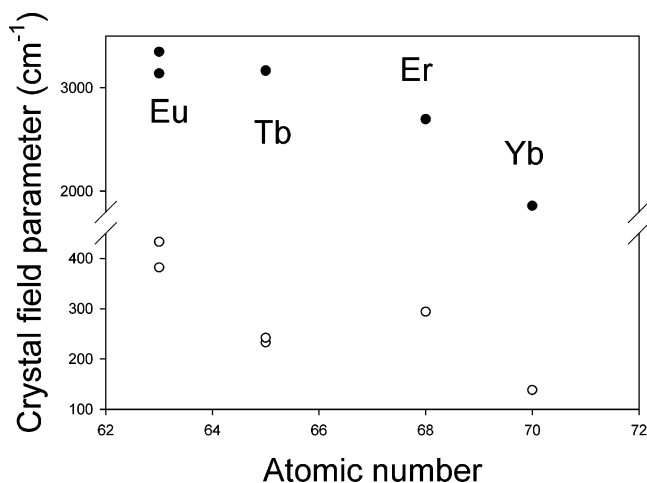

Figure 3. Crystal field parameters (top, B_0^4; bottom, B_0^6) for Cs_2-NaLnF$_6$ from standard 4f^N energy level fits as a function of atomic number of Ln. Note the scale break. (Data: Ln = Eu from refs 5 and 6 for Cs_2NaYF_6:Eu^{3+}; Tb from refs 12 and 13; Er from this work; Yb from ref 14).

cm^{-1} (and the standard deviations are 31 and 9.3 cm^{-1}) in the standard and CIACF analyses, respectively, so that the latter analysis greatly improves the energy level fitting.

The parameter sets are reported in Table 3 and are compared with that for $Cs_2NaErCl_6$. The main differences between the fluoride and the chloride parameter sets lie in the values of γ (40% lower for the fluoride), the three-body parameter T^2 (2.5

TABLE 3: Free-Ion and Crystal Field Parameters (in cm^{-1}) of Er^{3+} in Cs_2NaErF_6 and $Cs_2NaErCl_6$. The Values between Square Brackets were Held Constant. Standard Deviations are Given between Parentheses

	$Cs_2NaErCl_6$		Cs_2NaErF_6	
parameter	standard analysis	CIACF	standard analysis	CIACF, Table 1
F_2	96069(120)	96909(57)	97398(269)	97641(73)
F_4	66936(291)	67607(135)	68093(377)	68167(119)
F_6	49012(356)	50620(167)	55532(422)	55984(137)
α	17.80(0.3)	17.48(0.13)	18.4(1.4)	17.44(0.4)
β	−683(12)	−644(6)	−570(34)	−564(10)
γ	2493(106)	2279(50)	1631(122)	1682(41)
T^2	124(3)	172(2)	451(11)	490(4)
T^3	49(8)	43(4)	61(14)	41(4)
T^4	49(8)	78(4)	100(30)	113(9)
T^6	−337(18)	−282(8)	−245(110)	−193(34)
T^7	164(21)	225(9)	305(67)	256(20)
T^8	315(33)	277(13)	[160]	[160]
M^0	4.3(0.3)	4.8(0.1)	3.6(0.5)	4.4(0.2)
P^2	586(28)	870(15)	653(50)	903(42)
ζ (4f)	2327(2)	2292(0.9)	2308(16)	2283(5)
B_0^4 (4f4f)	1555(46)	944(23)	2696(81)	2156(50)
B_0^6 (4f4f)	154(18)	55(9)	294(27)	189(12)
$E'_{ave} − E_{ave}$		[80199]		[82000]
X		0.144(0.007)		0.267(0.002)
ζ (np)		[4154]		[500]
B_0^4 (4fnp)		−10244(98)		−9387(455)
N	75	75	39	39
n_p	18	21	17	20
σ	21.7	10.3	23.0	6.5
sd	24.9	12.1	30.6	9.3

TABLE 4: Percentage Admixture of 4f^{12}np^5 States in $Cs_2NaErCl_6$ and Cs_2NaErF_6

energy (cm^{-1})	4f^{11} wavefunction	4f^{12}np^5 wavefunction	admixture	
			$Cs_2NaErCl_6$	Cs_2NaErF_6
39 000	$^4D_{7/2}$	$^4I_{15/2}$	1.5	0.9
40 700	$^2I_{11/2}$	$^2D_{5/2}, ^2F_{7/2}$	0.7	-
41 000	$^2L_{17/2}$	$^2G_{9/2}, ^2H_{11/2}$	1.9	0.8
43 000	$^2I_{13/2}$	$^2D_{5/2}, ^2F_{7/2}, ^2I_{13/2}$	1.0	0.4
46 000	$^4D_{1/2}$	$^4I_{9/2}$	0.4	0.3
47 000	$^2L_{15/2}$	$^2G_{7/2}$	1.8	0.5
51 000	$^2H_{11/2}$	$^2H_{9/2}$	0.3	0.4

times stronger) and the crystal field parameters (about twice as strong). B_0^4 (4f4f) falls to 60% of its value from the standard analysis when the CIACF is applied to the chloride and to 80% of its value in the case of the fluoride. Referring to the B_0^4 (4f4f) value in the standard 4f^{11}2p^6 calculation, B_0^4 (4fnp) climbs to 6.6 times that value in the CIACF calculation for the chloride, and to 3.5 times that value in the case of the fluoride. The 4f^{11} wavefunctions of $Cs_2NaErCl_6$ and Cs_2NaErF_6 contain a certain amount of 4f^{12}np^5 (n = 3, 2, respectively) states. These amounts are reported in Table 4 and are rather smaller for the fluoride than for the chloride thus suggesting a lower configuration interaction. Besides, considering its expression in eq 19 of ref 11, the parameter γ reflects the perturbation of all the possible atomic interactions of 4f^{11} with 4f^9 l^2 (where l is s,p,d...etc.) Because it is less important for the fluoride also seems coherent with a lower configuration interaction with the ligand shell.

4. Conclusions

The electronic absorption and emission spectra of Cs_2NaErF_6 exhibit rich vibronic structure that has permitted the assignment of 39 crystal field energy levels. Although our analysis is consistent with that for $Cs_2NaErCl_6$, it is not as complete because the ultraviolet absorption spectra of Cs_2NaErF_6 are complex and assignments are ambiguous. One method to elucidate these higher energy levels would be to employ high-resolution excited-state absorption at low temperature.

In Figure 3, the derived fourth- and sixth-order crystal field parameters from various energy level parametrizations of Cs_2NaLnF_6 are plotted against the atomic number of Ln. Because only the hexafluoroelpasolite data for Er and Yb are available for CIACF fits, the data employed in the table is from the standard $4f^N$ fits. There is an overall decrease for both crystal field parameters when going from Ln = Eu to Yb. The major contributing factor to this decrease is envisaged to be the radial integrals, which are contained within the crystal field parameters.

References and Notes

(1) Tanner, P. A. *Top. Curr. Chem.* **2004**, *241*, 167.

(2) Becker, R.; Lentz, A.; Sawodny, W. *Z. Anorg. Allg. Chem.* **1976**, *420*, 210.

(3) Bucher, E.; Guggenheim, H. J.; Andres, K.; Hull, G. W.; Cooper, A. S. *Phys. Rev. B* **1974**, *10*, 2945.

(4) Urland, W. *Z. Naturforsch., A: Phys. Sci.* **1979**, *34*, 1507.

(5) Tanner, P. A.; Liu, Y. -L.; Edelstein, N.; Murdoch, K.; Khaidukov, N. M. *J. Phys.: Condens. Matter* **1997**, *9*, 7817.

(6) Thorne, J. R. G.; Jones, M.; McCaw, C. S.; Murdoch, K. M.; Denning, R. G.; Khaidukov, N. M. *J. Phys.: Condens. Matter* **1999**, *11*, 7851.

(7) Berry, A. J.; Morrison, I. D.; Denning, R. G. *Mol. Phys.* **1998**, *93*, 1.

(8) Makhov, V. N.; Khaidukov, N. M.; Lo, D.; Krupa, J. C.; Kirm, M.; Negodin, E. *Opt. Mater.* **2005**, *27*, 1131.

(9) Faucher, M. D.; Tanner, P. A. *Mol. Phys.* **2003**, *101*, 983.

(10) Tanner, P. A.; Mak, C. S. K.; Faucher, M. D. *J. Phys. Chem. A* **2004**, *108*, 5278.

(11) Rajnak, K.; Wybourne, B. G. *Phys. Rev.* **1963**, *132*, 280.

(12) Berry, A. J.; McCaw, C. S.; Morrison, I. D.; Denning, R. G. *J. Lumin.* **1996**, *66−67*, 272.

(13) Berry, A. J.; Morrison, I. D.; Denning, R. G. *Mol. Phys.* **1998**, *93*, 1.

(14) Zhou, X. -J.; Reid, M. F.; Faucher, M.; Tanner, P. A. *J Phys. Chem. B* **2006**, *110*, 14939.